Kinetic electron emission from Al surfaces by slow ions

M. Minniti,[1] M. Commisso,[1] A. Sindona,[1] E. Sicilia,[2] A. Bonanno,[1] P. Barone,[1] R. A. Baragiola,[3] and P. Riccardi[1,*]
[1]*Laboratorio IIS, Università della Calabria and INFN-Gruppo Collegato di Cosenza-87036 Rende, Cosenza, Italy*
[2]*Dipartimeto di Chimica, Università della Calabria-87036 Rende, Cosenza, Italy*
[3]*Laboratory for Atomic and Surface Physics, Department of Engineering Physics, University of Virginia, Charlottesville, Virginia 22904, USA*
(Received 30 November 2006; published 19 January 2007)

We measured energy distributions of electrons emitted in the interaction of Na^+ with Al surfaces at incident ion energies in the range 150–4000 eV. The data allow to correlate emission intensities with spectral signatures of electron excitation processes. We find a remarkable contribution to electron emission from asymmetric collisions between incoming ions that have survived neutralization at the surface and target atoms, leading to Al-2*p* excitation via a vacancy transfer process. We observe that the total electron emission yields sharp increases by more than an order of magnitude at impact energies above the threshold for this process.

DOI: 10.1103/PhysRevB.75.045424 PACS number(s): 79.20.Rf, 34.50.Dy, 68.49.Sf, 73.20.Mf

I. INTRODUCTION

Kinetic electron emission (KEE) in the interaction of slow atomic particles with metal surfaces, i.e., the emission of electrons at the expense of the kinetic energy of incoming projectiles, has been intensely investigated,[1] but still new mechanisms are being identified or proposed.[2–8]

KEE can occur by excitation of solid valence electrons in binary projectile-electron collisions in an idealized Fermi electron gas.[1] Energy and momentum conservation determine the threshold impact energy for this process. Below this threshold, subthreshold emission can occur by electron promotion in close atomic collisions.[9] Electron promotion processes are also characterized by well-defined thresholds, which depend on the particular combination of collision partners and can be experimentally determined and theoretically estimated from molecular orbital (MO) correlation diagrams.

Other subthreshold processes[2–5] have been recently investigated to understand nonvanishing electron emission observed at impact energies below the threshold for electron promotion. Research on KEE below the threshold for promotion is just beginning. Experiments of singly charged ions impacting metal surfaces at normal or near normal incidence[2–5] showed that electron emission yields decrease exponentially with the reciprocal of projectile velocity. Theoretical interpretations of these observations have been attempted, considering either nonadiabatic one-electron excitations or many-electron interactions,[5] but the basic understanding of the underlying mechanisms is still insufficient to draw definitive conclusions.

Studies of KEE are often performed under sufficiently selective experimental conditions to isolate the effect under consideration, or focus on individual processes revealed by the experiments. Although this clarifies the basic physics of each emission mechanism, it leaves open the question of the interplay between different electron excitation and emission phenomena, as testified by the current debate[2–5,10,11] about the competition of electron promotion and the other subthreshold processes. Furthermore, besides the primary excitation events, it has to be considered that secondary effects, such as bulk plasmon excitation and electronic and atomic collision cascade, make it more difficult to establish the role of different basic excitation mechanisms.

In this work, we deal with the complexity of the interactions leading to electron emission induced by atomic particles by studying electron emission in the interaction of 150–4000 eV Na^+ ions with Al surfaces. For this projectile-target system, several emission processes are known to occur, including inner shell excitation of projectiles and target atoms,[12–14] bulk plasmon excitation,[8,15] and emission below the promotion threshold.[2–5] Our goal is to clarify the role of the observed emission mechanisms when they concur in determining the behavior of electron emission yields[16,17] with incoming ion velocity. Indeed, since the measurements of Alonso *et al.*,[16] this question has not yet been fully elucidated, and efforts in this direction have been undertaken only recently.[10,11,15] We find that electron emission is dominated by electron-promotion processes, while the other subthreshold processes[5] appear to be relevant only at impact energies for which promotion is not operative. For the Na^+-Al system, electron promotion occurs either in binary collisions between the projectile and a target atom (asymmetric collisions) and between a fast recoil and another target atom (symmetric collisions). Asymmetric collisions involve either projectiles that have been neutralized in the interaction with the surface[18] and survived ions.

A striking result of the present experiments is the finding of a significant contribution of asymmetric collisions involving survived ions to the total electron emission yield. This result is surprising because of high neutralization rates for slow ions at metal surfaces. We observe that the intensity of electron emission increases sharply by more than an order of magnitude above a threshold impact energy of about 450 eV, being correlated to a vacancy transfer process[19,20] that produces L-shell excitation in Al atoms in asymmetric collisions involving projectile ions, below the threshold for L-shell excitation in target Al-Al symmetric collision. This result implies that KEE induced by ions can be substantially different from that induced by neutral projectiles and that surface neutralization and charge-transfer processes may have a significant role in KEE from the metal surface.

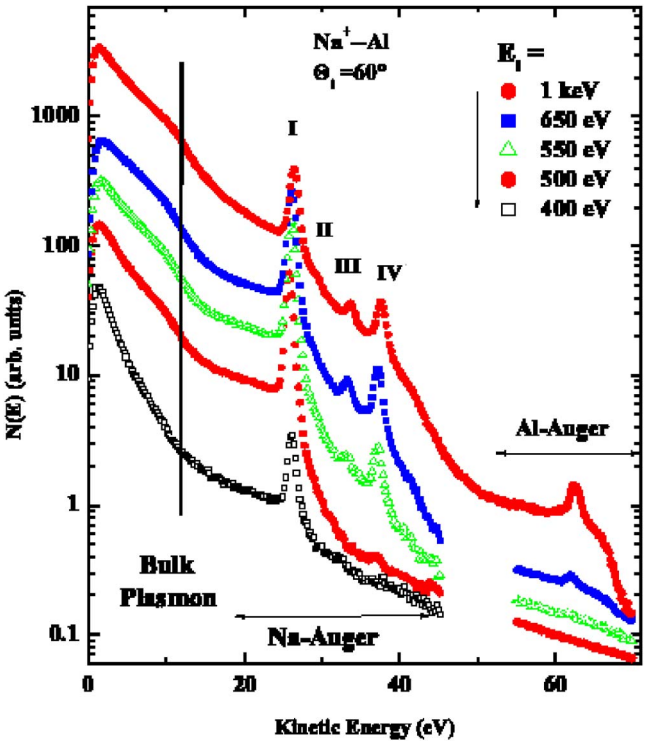

FIG. 1. (Color online) Energy spectra of electrons emitted from the Al surfaces under the impact of Na^+ ions at varying incident ion energy for fixed incidence angle $\Theta_i=60°$. The spectra have been arbitrarily displaced on the vertical scale for clarity.

II. EXPERIMENTS

Details of the experimental setup have been described previously.[8] Experiments were performed in an ultrahigh-vacuum (UHV) chamber with a base pressure of 3×10^{-10} Torr. Na^+ ions were produced with a Kimball Physics ion gun. The ion beam current was of the order of 10^{-9} A and had a Gaussian spatial distribution in both horizontal and vertical directions, as measured with a movable Faraday cup situated in the target position.

The energy distributions of emitted electrons was measured by either a fixed hemispherical energy analyzer situated at 60° from the beam direction [spectra in Fig. 1(a)] or by another hemispherical analyzer mounted on a rotatable goniometer [Fig. 1(b)]. These analyzers, lying in the incidence plane, had semiacceptance angles of 25° and 1.5° and were operated at a constant pass energy ($\Delta E=40$ and 50 eV, respectively).

The polycrystalline Al samples (purity 99.999%) was sputter cleaned by 6 keV Ar^+ bombardment. Sample cleanness was assured by the absence of oxygen, carbon, and sodium signals in electron-induced Auger spectroscopy performed right before and after the acquisition of each spectrum and by the constancy of the energy position of sodium Auger lines during each spectral scan.

III. RESULTS

Figure 1 reports energy distributions of electrons emitted from an Al surface bombarded by Na^+ ions at varying energy, for an incident angle $\theta_i=60°$ and an observation angle $\theta_e=0°$ (both measured with respect to the surface normal). Figure 2 reports the results of measurements performed at varying incidence angle for a fixed impact energy of 300 eV and observation angle $\theta_e=0°$. The spectra show evidence for several kinetic emission phenomena. The structure in the 10–15 eV energy range is attributed to electron emission from bulk plasmon decay.[8,10,15,21] Figure 1(a) shows several narrow peaks labeled I–IV in the 20–45 eV energy range. The narrow width of these peaks (~1 eV) is typical of atomic transitions, indicating that they result from the Auger decay in vacuum of reflected sodium projectiles that have $2p$ shell vacancies created by electron promotion in a binary collision with Al target atoms. Attribution of the main atomic features appearing in the spectra (reported in Table I for completeness) has already been discussed in Ref. 18 and is consistent with calculations.[22]

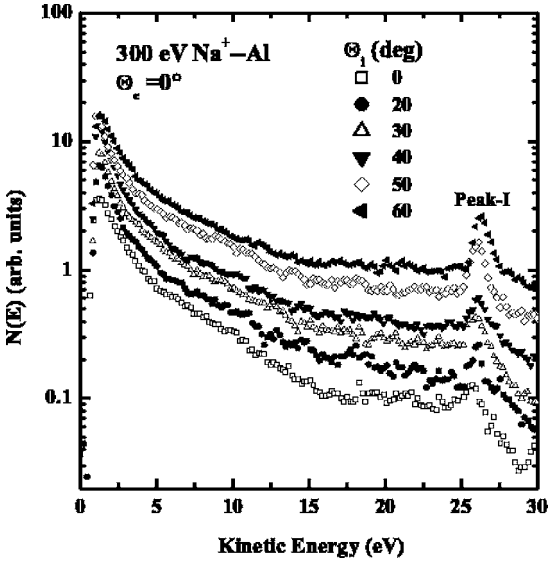

FIG. 2. Energy spectra as a function of Θ_i for fixed incident ion energy $E_i=300$ eV and observation angle $\Theta_e=0°$.

In the 55–70 eV energy range, we observe atomic peaks due to Al LMM-Auger transitions in sputtered excited atoms,

TABLE I. Sodium Auger transition lines and assignment.

Label	Experimental energy	Expected energies	Initial state	Final state
I	25.7	25.7[a]	$2p^5 3s^2$	$2p^6$
II	28.5	28.9[a]	$2p^5 3s 3p(^1P)$	$2p^6$
		Or		
		28.7[a]	$2p^4(^3P)3s^2$	$2P^5$
III	32.9	32.6[a]	$2p^4(^1D)3s^2$	$2p^5$
IV	37.0	37.2[b]	$2p^4 3p 3s$	$2p^5$
V	41.3[c]	41.4[a]	$2p^4(^1D)3s^2 3p$	$2p^5 3s$

[a]From Ref. 9.
[b]$Z+1$ rule.
[c]Line V is very weak and not discernible in the present experimental conditions. It has been observed in Ref. 21.

superimposed on a broad structure due to Al LVV-Auger transitions of excited atoms decaying inside the solid and involving two valence electrons.[1,9,13,15] This region of the spectrum has been acquired separately, since the statistical quality of our spectra is limited by the short acquisition time and the low beam currents needed to prevent significant contamination of the sample by the Na beam, especially at the thresholds for the observation for the Auger signals.

IV. DISCUSSION

A. Sodium 2*p* excitation

We notice that peaks II-IV are observed at impact energies above a threshold value of about 450 eV. This observation further supports the assignment of these peaks, given in Ref. 18 in analogy with the case Ne^+ impact, to the decay of doubly excited sodium projectiles due to simultaneous promotion of two $2p$ electrons in binary collisions between target atoms and incoming ions which have survived neutralization processes in the interaction with the surface. In fact, the ground state configuration of a Na^+ ions is the same of Ne atoms and, therefore, collisions involving incoming ions produce both the $2p^5$ and the $2p^4$ excited states with the same threshold energy. On the other hand, at impact energies lower than 450 eV, the structures due to the decay of the singly excited $2p^5$ states are the only atomic features appearing in the spectra. This implies that the observed structures are due to the decay of sodium projectiles that have been resonantly neutralized in the incoming trajectory, before the hard collision with a target atom. In fact, the absence of structures due to decay of doubly $2p$ excited states excludes contribution to the Auger spectrum of sodium collisions involving survived ions, which require a smaller closest approach distance for $2p$ level promotion and, therefore, a higher threshold energy. This interpretation of the observed Auger spectrum of sodium is further supported by calculations of MO correlation diagrams, performed for the collisional systems Na-Al and Na^+-Al and reported in Figs. 3 and 4, respectively. These diagrams were calculated using the density functional theory (DFT) method in the B3LYP formulation[23,24] using the computer code GAUSSIAN 03.[25] All electron basis sets[26] of double-zed (DZVP) quality for Na and Al were used to construct the diagram point by point, i.e., adiabatically. We notice that the results of the calculations appear to be nicely consistent with published MO diagrams for Ne-Al collisions.[27] In a fast collision, the electronic system cannot evolve adiabatically and electronic transitions can occur at the expense of the kinetic energy of incoming particles at the adiabatically forbidden crossings between MOs. The diabatic promotion path can therefore be constructed from the adiabatic correlation diagram, as indicated by the dashed lines in Figs. 3 and 4, showing the well-known promotion of the 6σ ($4f\sigma$) MO correlated to the projectile's $2p$ level in the separate atom limit. We observe that, for binary collisions of neutrals Na with Al atoms, the first forbidden crossing occurs at about 1.3 a.u., whereas the promotion path in the case of Na^+-Al is shifted to lower internuclear distances, consistent with our observations.

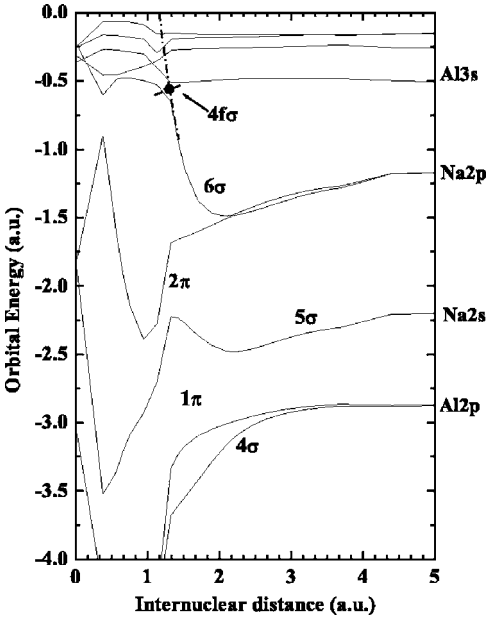

FIG. 3. Adiabatic MO correlation diagrams for the selected orbitals of Na-Al as calculated by the DFT method. The levels for the separated-atom limit are indicated on the right-hand side of the diagram. The dashed-dotted heavy curve shows the promotion of diabatic levels into continuum. The adiabatic levels are labeled in the MO notation. The lowest orbital of a given symmetry is numbered 1, and numbering continues in ascending order up to higher energies.

B. Emission intensities

Mechanisms for kinetic electron emission have been recently studied[2–5] by plotting the electron emission yields as a function of $1/v$, the inverse of the velocity of incoming projectiles. Figure 5 depicts the intensity of electron emission,

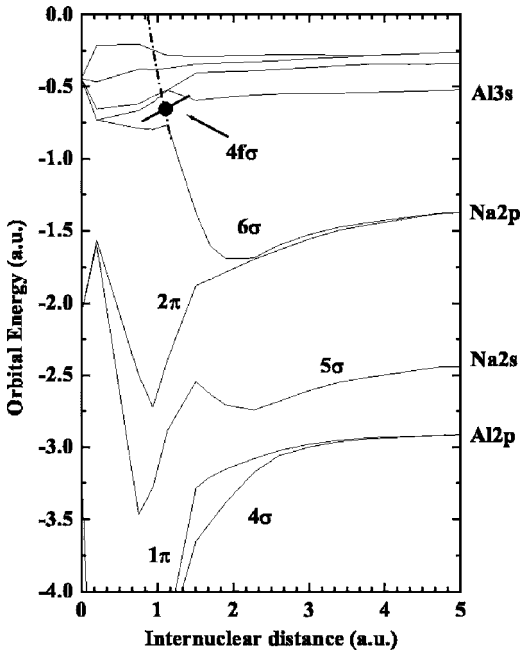

FIG. 4. Same as Fig. 3 but for Na^+-Al.

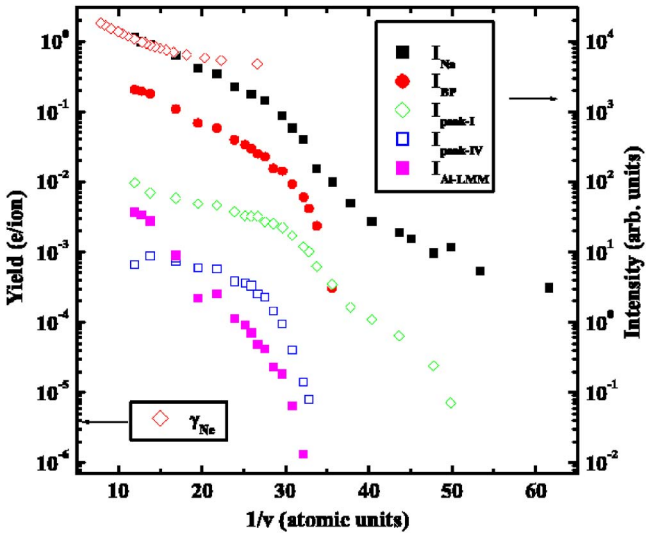

FIG. 5. (Color online) Intensities of electron emission for Na^+ ions vs v^{-1}, the inverse of the velocity of incoming ions. I_{Na} is the area of the spectra revealed for $\Theta_i=60°$. I_{BP} is the area of the plasmon feature. $I_{Al\text{-}LMM}$, I_I, and I_{IV} are the areas of the Al-Auger peak and of the main sodium peaks I and IV, respectively, reported after background subtraction. For comparison is reported γ_{Ne}, the yield of electron emission induced by Ne^+ for $\Theta_i=60°$.

I_{Na}, vs $1/v$ together with the intensities of the main sodium atomic peaks, Na-I and Na-IV, of the Al-LMM structure (after background subtraction) and of the plasmon decay feature. The intensity of electron emission from plasmon decay is obtained using different methods of data analysis reported in previous works by us and other authors.[10,28,29]

We remark on two noticeable aspects of Fig. 5: (i) all the curves increase significantly for $1/v$ lower than a threshold value of about 35 a.u., closely corresponding to 450 eV impact energy; (ii) at higher velocities, the total electron yields, the plasmon decay, and the Al-Auger intensities follow a similar trend but different from that of the structures due to projectile excitation. The correlation between the intensity of electron emission from plasmon decay and from Al-Auger, including their threshold behavior, and the total electron emission yield is consistent with previous results obtained for noble gas ions[10,15] (see the behavior of the electron emission yields γ_{Ne} for Neon ion impact,[16,17] reported in Fig. 5 for comparison), indicating that fast Auger electrons are efficiently scattered inside the solids, initiating electronic collision cascades that produce plasmons and secondary electrons. This implies that electron promotion leading to the excitation of Al target atoms plays the dominant role in kinetic electron emission from Al surfaces. In particular, we observe that the threshold energy for the observation of the Al-Auger signal is lower than the threshold energy for excitation in target Al-Al symmetric collisions[13] and is very similar to the threshold for the observation of Na II-IV peaks. This suggests that the L-shell vacancy in the target Al atoms can be created also in asymmetric collisions with the lighter Na projectiles. A plausible mechanism is that one of the L-shell vacancies present in the Na $2p^4$ can be transferred to the Al collision partner via a two electron *autoexcitation* mechanism, similar to that observed in the case of Ne^+-Al and other systems.[19,20] In this process, an external electron of Na fills a $2p$-Na vacancy, while a $2p$-Al electron is promoted in the $2p$-Na vacancy, going from the $Na^+2p^43s^2$ (or Na^+2p^43s3p) $+Al2p^63s^23p$ configuration to the $Na2p^63s+Al^+2p^53s^23p$ configuration. The correlation diagram of Fig. 4 shows that the process is energetically possible in the receding path over a wide range of internuclear distances.

For Ne^+ ions, γ_{Ne} significantly levels off at low velocities due to potential electron emission, masking kinetic electron emission mechanisms. This does not occur for sodium projectiles, which do not carry sufficient potential energy, and therefore allows studying the evolution of kinetic electron emission in the investigated energy range. At impact velocities below the Al-LMM threshold, the intensity of peak I decreases, showing a similar threshold. On the other hand, the total electron emission yield γ_{Na} does not show any definite threshold, approaching an exponentially decreasing trend with $1/v$, consistent with recent experimental observations.[2–5] This implies the existence also of emission below the promotion threshold. The competition between the two processes is clarified by the measurements made as a function of incidence angle. For discussion of the angular measurements, it is important to specify that Figs. 1 and 2 show a broad feature underlying peak I and extending up to about 6–7 eV around this peak. Evaluation of the intensity of this structure appears to be strongly dependent on the subtraction of the background spectrum. Nevertheless, we find[30] that the intensity of this structure and peak I have similar dependence on projectile energy, suggesting that they originate in the same excitation mechanisms. Furthermore, the ratio between the intensities of the two structure results is independent of the electron emission angle θ_e,[30] allowing us to rule out Auger decay inside the bulk of excited Na atoms as a possible assignment for the broad feature, since in this case this ratio should increase as $(\cos\theta_e)^{-1}$. A similar structure was observed also in the case of a Neon projectile,[12] tentatively attributed to an Auger deexcitation process involving an electron from the solid. More likely, as discussed in Ref. 14, the broad feature results from atomic decay closer to the surface, where distance-dependent shift and broadening of atomic energy levels due to the atom-surface interaction may influence the spectrum produced by the Auger decay of Na atoms excited in the $2p^53s^2$ state, resulting in the observation of this structure. On the other hand, peak I results from excited atoms scattered at larger angles and therefore decaying farther away from the surface. On rough surfaces,[14] the observation of peak I is therefore favored when the impact direction is moved away from the (macroscopic) surface normal, consistent with the observations reported in this work and previously.[14]

The results of the angular measurements shown in Fig. 6 indicate that the intensity of electron emission is similar to the intensity of the Auger features observed in the spectra, leading to the conclusion that at 300 eV the emission is dominated by electronic excitations resulting from binary atomic collisions, similar to those that are clearly signaled by the observed Na Auger spectrum.

V. CONCLUDING REMARKS

Our experiments give a detailed account for the mechanisms of kinetic electron emission from Al surfaces, estab-

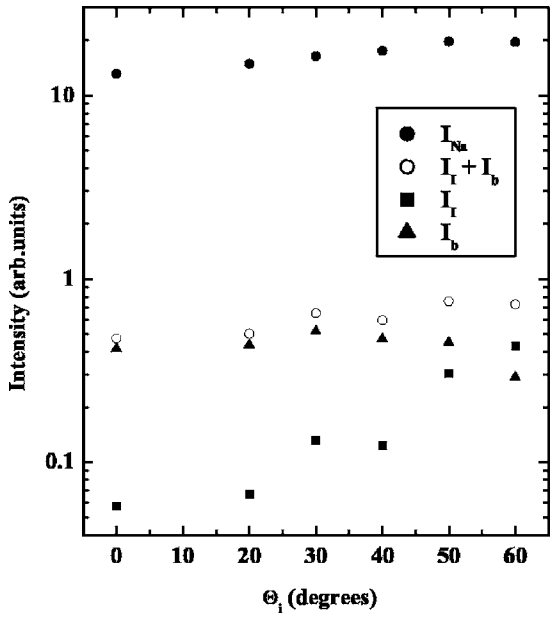

FIG. 6. Intensities of electron emission vs Θ_i for fixed impact energy E_i=300 eV and Θ_e=0°. I_{Na} and I_I are the same as in Fig. 5. I_b is the area of the broad feature underlying peak I.

lishing the role of each emission process observed in the spectra of emitted electrons. The results show the contribution to KEE from Al surfaces under Na^+ impact given by a vacancy-transfer process that produces Al-2*p* excitation in asymmetric collisions involving survived ions. We would like to point out some consequences of our findings that may be important for future investigations:

(i) KEE can be significantly influenced by the actual charge state of incoming particles at the moment of collision and that KEE induced by singly charged ions may be substantially different from that induced by neutrals. Studies of KEE have been recently reported in the case of Neon impact on Al surfaces[6,11] using neutral projectiles to exclude contribution from potential electron emission[18] arising in the case of ion impact. The results of our work can be easily extended to the case of neon impact. In fact, in this case, formation of projectile triply excited states correlated to Al 2*p* excitation have been reported for ion impact but not for neutrals.[11,12,20]

(ii) Charge-transfer processes, when present, need to be accounted for in the discussion of the intensity of electron emission. Furthermore, the Al atoms excited by these processes can be sputtered from the solid and their Auger decay can occur in vacuum, as testified by the observation of narrow Al-LMM Auger lines. Therefore, our experiments show evidence that these charge-transfer processes can also have a significant effect in the formation of sputtered ion species, a longstanding issue in secondary ion mass spectroscopy (SIMS).[31]

(iii) The complex interplay between different excitation mechanisms in most cases cannot be neglected. Theoretical calculations have neglected the role of electron promotion, even in cases where it should be efficient, such as in experiments of Na^+ bombardment of Ru surfaces contaminated by different amounts of adsorbed sodium atoms.[4,5] In contrast, in experiments of Ne^+ bombardment of metal surfaces contaminated by adsorbed sodium atoms, projectiles, and target autoionization lines were observed since the very initial stages of adsorption.[32] In particular, sodium excitation is due to a vacancy-sharing process and to electron promotion in symmetric collisions between Na target atoms at low and high coverage, respectively. Therefore, depending on the amount of adsorbed Na, we expect a significant contribution of electron promotion also in the case of Na^+ bombardment of Ru surfaces modified by Na adsorbates.[4,5]

ACKNOWLEDGMENT

Helpful discussions with Z. Sroubek and J. Lorincik are gratefully acknowledged.

*Corresponding author. Electronic address: riccardi@fis.unical.it

[1] R. A. Baragiola, in *Low Energy Ion Surface Interaction*, edited by J. W. Rabalais (Wiley, New York, 1994), Chap. 4.
[2] J. Lorincik, Z. Sroubek, H. Eder, F. Aumayr, and H. P. Winter, Phys. Rev. B **62**, 16116 (2000).
[3] J. A. Yarmoff, T. D. Liu, S. R. Qiu, and Z. Sroubek, Phys. Rev. Lett. **80**, 2469 (1998).
[4] J. A. Yarmoff, H. T. Than, and Z. Sroubek, Phys. Rev. B **65**, 205412 (2002).
[5] Z. Sroubek, X. Chen, and Y. Yarmoff, Phys. Rev. B **73**, 045427 (2006).
[6] H. P. Winter, S. Lederer, H. Winter, C. Lemell, and J. Burgdorfer, Phys. Rev. B **72**, 161402(R) (2005).
[7] G. Spierings, I. Urazgil'din, P. A. Zeijlmans van Emmichoven, and A. Niehaus, Phys. Rev. Lett. **74**, 4543 (1994).
[8] P. Riccardi, P. Barone, A. Bonanno, A. Oliva, and R. A. Baragiola, Phys. Rev. Lett. **84**, 378 (2000).
[9] M. Barat and W. Lichten, Phys. Rev. A **6**, 211 (1972).
[10] M. Commisso, M. Minniti, A. Sindona, A. Bonanno, A. Oliva, R. A. Baragiola, and P. Riccardi, Phys. Rev. B **72**, 165419 (2005).
[11] Y. Matulevich, S. Lederer, and H. Winter, Phys. Rev. B **71**, 033405 (2005).
[12] F. Xu, N. Mandarino, A. Oliva, P. Zoccali, M. Camarca, A. Bonanno, and R. A. Baragiola, Phys. Rev. A **50**, 4040 (1994).
[13] N. Mandarino, P. Zoccali, A. Oliva, M. Camarca, A. Bonanno, and F. Xu, Phys. Rev. A **48**, 2828 (1993).
[14] O. Grizzi, E. A. Sanchez, J. E. Gayone, L. Guillemot, V. A. Esaulov, and R. A. Baragiola, Surf. Sci. **469**, 71 (2000).
[15] N. Bajales, S. Montoro, E. C. Goldberg, R. A. Baragiola, and J. Ferron, Surf. Sci. **579**, L97 (2004).
[16] E. V. Alonso, R. A. Baragiola, J. Ferron, M. M. Jakas, and A. Oliva-Florio, Phys. Rev. B **22**, 80 (1980).
[17] K. Wittmack, Nucl. Instrum. Methods Phys. Res. B **115**, 288 (1996).
[18] H. D. Hagstrum, in *Inelastic Ion-Surface Collisions*, edited by N. H. Tolk, J. C. Tully, W. Heiland, and C. W. White (Academic

Press, New York, 1977).
[19] N. Stolterfoht, Phys. Rev. A **47**, R763 (1993).
[20] F. Xu, N. Mandarino, A. Oliva, P. Zoccali, M. Camarca, and A. Bonanno, Nucl. Instrum. Methods Phys. Res. B **90**, 564 (1994).
[21] M. Commisso, A. Bonanno, A. Oliva, M. Camarca, F. Xu, P. Riccardi, and R. A. Baragiola, Nucl. Instrum. Methods Phys. Res. B **230**, 438 (2005).
[22] P. Dahl, M. Rodbro, G. Hermann, B. Fastrupp, and M. E. Rudd, J. Phys. B **9**, 1581 (1976).
[23] A. D. Becke, J. Chem. Phys. **98**, 5648 (1993).
[24] P. J. Stephens, F. J. Devlin, C. F. Chabalowski, and M. J. Frisch, J. Phys. Chem. **98**, 11623 (1994).
[25] M. J. Frisch *et al.*, GAUSSIAN 03, rev. A.1 (Gaussian, Inc., Pittsburgh, PA, 2003).
[26] N. Goudbout, D. R. Salahub, J. Andzelm, and E. Wimmer, Can. J. Chem. **70**, 560 (1992).
[27] J. Lorincik and Z. Sroubek, Nucl. Instrum. Methods Phys. Res. B **164-165**, 633 (2000).
[28] N. Stolterfoht, D. Niemann, V. Hoffmann, M. Rosler, and R. A. Baragiola, Phys. Rev. A **61**, 052902 (2000).
[29] D. A. Shirley, R. A. Martin, S. P. Kowalczyk, F. R. McFeely, and L. Ley, Phys. Rev. B **15**, 544 (1977).
[30] P. Barone, A. Bonanno, M. Commisso, M. Minniti, A. Oliva, and P. Riccardi, Radiat. Phys. Chem. (to be published).
[31] X. Chen, Z. Sroubek, and Y. Yarmoff, Phys. Rev. B **73**, 132408 (2006).
[32] P. Zoccali, A. Bonanno, M. Camarca, A. Oliva, and F. Xu, Phys. Rev. B **50**, 9767 (1994).